

A VISCOELASTIC VOF-PROST CODE FOR THE STUDY OF DROP DEFORMATION

Y. and M. Renardy*
T. Chinyoka

Department of Mathematics
Virginia Tech
Blacksburg VA 24061-0123
Email: renardy@math.vt.edu

D. B. Khismatullin

Department of Biomedical Engineering
Duke University
Durham NC 27708

J. Li

Engineering Department,
University of Cambridge
Maddingley Road
Cambridge CB30EZ
UK

ABSTRACT

A volume of fluid method is developed with a parabolic representation of the interface for the surface tension force (VOF-PROST). This three-dimensional transient code is extended to treat viscoelastic liquids with the Oldroyd-B constitutive equation. Simulations of deformation for a Newtonian drop in a viscoelastic medium under shear are reported.

INTRODUCTION

Emulsions arise in a wide range of industrial applications: in materials processing, waste treatment, pharmaceuticals, and incompatible polymer blends for recycling plastics. There are several broad categories for making emulsions, but due to a fundamental lack of understanding of the processes, many of the industrial products are made by trial and error [1]. In order to predict and control these processes, a starting point is to consider the deformation and breakup behavior of single droplets within another liquid in a well-defined flow field. We focus on simple shear.

The evolution of a Newtonian two-dimensional drop (cylinder) sheared in another liquid was investigated in Ref. [2, 3]. The case of a Newtonian drop breaking under shear in another Newtonian liquid was treated numerically in Refs. [4, 5, 6, 7, 8]. The case of a two-dimensional drop of an upper-convected Maxwell liquid in a Newtonian matrix in time-periodic extensional flow was examined with a front-tracking method in Ref. [9]. Extension

and retraction of an Oldroyd-B drop in another liquid has been examined in [10] with a finite element method. In this paper, we show simulations for a Newtonian drop sheared in an Oldroyd B liquid and compare with experimental results of Ref.[11].

Volume-of-fluid (VOF) methods are popular for the direct numerical simulation of time-dependent viscous incompressible flow of multiple liquids. One weakness of past formulations appears when the capillary force is the dominant physical mechanism. The lack of convergence with spatial refinement, or convergence to a solution that is slightly different from the exact solution, has been documented in the literature. A well-known limiting case for this is the existence of spurious currents for the simulation of a spherical drop with zero initial velocity. Our algorithm VOF-PROST (a Parabolic Reconstruction Of Surface Tension for the volume-of-fluid method) effectively eliminates spurious currents[12, 13]. We report the extension to viscoelastic liquids and compare with results in the literature.

GOVERNING EQUATIONS

The momentum equation is

$$\rho \left(\frac{\partial \mathbf{u}}{\partial t} + \mathbf{u} \cdot \nabla \mathbf{u} \right) = \nabla \cdot \mathbf{T} - \nabla p + \text{div}(\eta(\nabla \mathbf{u} + (\nabla \mathbf{u})^T)) + \sigma \kappa \mathbf{n} \delta_S, \quad (1)$$

where σ denotes the surface tension coefficient, δ_S denotes the δ -function at the interface, κ denotes curvature, and \mathbf{T} is the extra

* Address all correspondence to these authors.

stress tensor. The total stress tensor is

$$\underline{\boldsymbol{\tau}} = -p\mathbf{I} + \mathbf{T} + \eta[\nabla\mathbf{u} + (\nabla\mathbf{u})^T]. \quad (2)$$

The densities of the two liquids are equal and denoted by ρ . The solvent viscosities are η_s , polymeric viscosities η_p , total viscosities $\eta = \eta_s + \eta_p$, relaxation times λ , and $G(0) = \eta_p/\lambda$.

The constitutive equation for the Oldroyd-B model is

$$\lambda\left(\frac{\partial\mathbf{T}}{\partial t} + (\mathbf{u} \cdot \nabla)\mathbf{T} - (\nabla\mathbf{u})\mathbf{T} - \mathbf{T}(\nabla\mathbf{u})^T\right) + \mathbf{T} = \lambda G(0)(\nabla\mathbf{u} + (\nabla\mathbf{u})^T). \quad (3)$$

The drop is initially spherical with radius a . The walls are located at $z = 0, L$. The initial condition is simple shear for the velocity and corresponding stresses for both the drop fluid and the matrix fluid. The velocity $(U(z), 0)$ is

$$U(z) = U_0 \frac{2z - L}{L}, \quad (4)$$

leading to a shear rate of

$$\dot{\gamma} = U'(z) = \frac{2U_0}{L}. \quad (5)$$

The constitutive law yields a quartic equation linking T_{13} to $\dot{\gamma}$; cf. Section 3.2 of [14] for details.

VISCOELASTIC PROST ALGORITHM

The discretized time integration scheme is

$$\lambda\left(\frac{\mathbf{T}^{(n+1)} - \mathbf{T}^{(n)}}{\Delta t} + (u^{(n)}\frac{\partial}{\partial x} + v^{(n)}\frac{\partial}{\partial y} + w^{(n)}\frac{\partial}{\partial z})\mathbf{T}^{(n+1)}\right) + \mathbf{T}^{(n+1)} = \lambda\left((\nabla\mathbf{u}^{(n)})\mathbf{T}^{(n)} + \mathbf{T}^{(n)}(\nabla\mathbf{u}^{(n)})^T - G(0)(\nabla\mathbf{u}^{(n)} + (\nabla\mathbf{u}^{(n)})^T)\right), \quad (\nabla\mathbf{u})_{ij} = \frac{\partial u_i}{\partial x_j}.$$

An Eulerian mesh of rectangular cells is used. The momentum equations are finite-differenced on a staggered mesh. The u -velocity is centered at the back face, the v -velocity at the left side face, and the w -velocity is centered at the bottom face of the cell. The pressure, $p_{i,j,k}$ and the color function $c(i, j, k)$ are located at the center. The diagonal components of the extra stress tensor take values at the center of the cell, while each off-diagonal component is at the mid-point of an edge.

Collecting the explicit terms to the right hand side, the constitutive equation is

$$\lambda\left(\mathbf{T}^{(n+1)} + \Delta t(u^{(n)}\frac{\partial}{\partial x} + v^{(n)}\frac{\partial}{\partial y} + w^{(n)}\frac{\partial}{\partial z})\mathbf{T}^{(n+1)}\right) + \Delta t\mathbf{T}^{(n+1)} = \lambda\left(\mathbf{T}^{(n)} + \Delta t((\nabla\mathbf{u}^{(n)})\mathbf{T}^{(n)} + \mathbf{T}^{(n)}(\nabla\mathbf{u}^{(n)})^T) + G(0)(\nabla\mathbf{u}^{(n)} + (\nabla\mathbf{u}^{(n)})^T)\right).$$

The left hand side is re-written

$$\left[\lambda\left(1 + \Delta t(u^{(n)}\frac{\partial}{\partial x} + v^{(n)}\frac{\partial}{\partial y} + w^{(n)}\frac{\partial}{\partial z})\right) + \Delta t\right]\mathbf{T}^{(n+1)}, \quad (6)$$

where the operator on $\mathbf{T}^{(n+1)}$ is approximated by

$$(\lambda + \Delta t)\left(1 + \frac{\lambda}{\lambda + \Delta t}u^{(n)}\Delta t\frac{\partial}{\partial x}\right)\left(1 + \frac{\lambda}{\lambda + \Delta t}v^{(n)}\Delta t\frac{\partial}{\partial y}\right) \times \left(1 + \frac{\lambda}{\lambda + \Delta t}w^{(n)}\Delta t\frac{\partial}{\partial z}\right) + O((\Delta t)^2).$$

The right hand side is coded for every i, j, k , at the center of the cell. That is, T_{12} is not simply the analogue of the Newtonian S_{12} , but is the average of such values taken at the four edges.

COMPARISON WITH EXPERIMENTAL DATA

The small deformation of a Newtonian drop in a Boger fluid undergoing slow steady shear was studied experimentally in [11]. Several fluid pairs were used.

The ratio of elastic stress to interfacial stress is

$$N = \frac{\Psi_1 \dot{\gamma}^2 a}{2\sigma}, \quad (7)$$

where Ψ_1 denotes the first normal stress difference coefficient. Non-Newtonian effects appear during deformation when N is comparable to Ca^2 . The higher the ratio N/Ca^2 , the more different the drop evolution as compared with the Newtonian counterpart. The highest value of N/Ca^2 in their paper is 4, for a matrix liquid with viscosity 10.3 Pa s, and a first normal stress difference coefficient $\Psi_1 = 7.5$ Pa s². The drop is a silicone oil with viscosity 1.12 Pa s. They name these fluids C1 and D2, respectively. The interfacial tension is 0.0013 N/m. The evolution with time of the Taylor deformation parameter

$$D = \frac{R_{\max} - R_{\min}}{R_{\max} + R_{\min}} \quad (8)$$

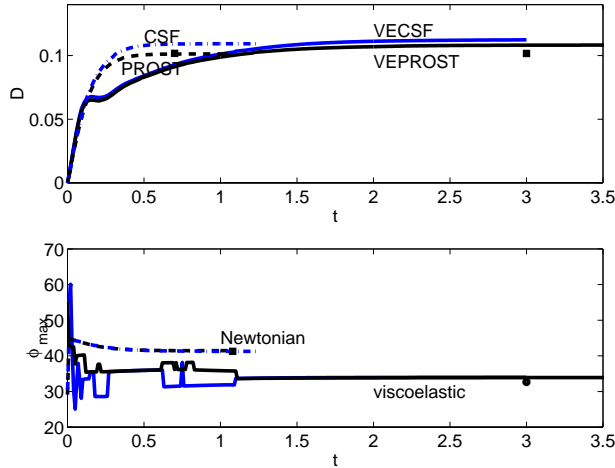


Figure 1. EVOLUTION OF DEFORMATION D AND ANGLE OF INCLINATION ϕ_{\max} AT $Ca = 0.1$. t IS MEASURED IN UNITS OF $\dot{\gamma}^{-1}$. THE C1-D2 RESULT IS SOLID, WITH 'o' DENOTING THE STATIONARY STATE FOR SMALL DEFORMATION THEORY. THE NEWTONIAN COUNTERPART IS DASHED, WITH THE SQUARE MARKING ITS SMALL DEFORMATION THEORY.

and the angle of inclination with the x-axis, ϕ_{\max} , are given in Fig. 8 of [11] for the range of capillary number up to 0.15. The vertical cross-sectional area through the center of the drop is fitted with an ellipse and R_{\max} and R_{\min} denote its major and minor axes, respectively [11].

At $Ca = 0.1$, for instance, the drop radius is $11.5 \mu\text{m}$ and the shear rate is $\dot{\gamma} = 1.0987 \text{ m/s}$. The perturbation theory of [15] for slow flow past a drop for second-order fluids gives $D = 0.1017$ and $\phi_{\max} = 32.625 \text{ deg}$. When the matrix liquid has no elasticity, the result is the same for D but the angle is $\phi_{\max} = 41.2706 \text{ deg}$. This provides a check for the numerical accuracy of our code for small deformations. Figure 1 shows our computational results. Spatial and temporal refinements were performed until D and ϕ_{\max} are converged to several digits: for this figure, this is achieved for a computational domain $[0, 8a] \times [0, 8a] \times [0, 8a]$, $\Delta x = \Delta y = \Delta z = a/16$, and $\Delta t = 0.0002\dot{\gamma}^{-1}$. Solid lines represent the C1-D2 pair, with 'o' denoting the stationary state for the small deformation theory of [11]. The Newtonian counterpart is dashed and the square represents the theoretical stationary solution for small deformation.

Table 1 is a comparison of the stationary solution. CSF refers to our Continuous Surface Force algorithm[16, 17, 18, 19, 20] and VECSF its viscoelastic version. In the codes, the angle of inclination is computed only to within the accuracy of a grid cell, and this accounts for the jumps in its value during the evolution. The mesh size for these results is $\Delta x = \Delta y = \Delta z = a/16$, and the timestep is $\Delta t = 0.0002\dot{\gamma}^{-1}$. A spatial convergence test for VEPROST (viscoelastic PROST) at a mesh size of $a/20$ for

Table 1. COMPARISON OF STATIONARY STATES FOR NUMERICAL AND SMALL DEFORMATION THEORY (sdt) FOR C1-D2 PAIR AT $Ca=0.05, 0.1, 0.14$. WE DENOTE $\% \Delta D$ AS THE PERCENTAGE DIFFERENCE OF THE DEFORMATION PARAMETER WITH THAT OF THE SMALL DEFORMATION THEORY $|D - D_{\text{small def.}}| \times 100/D_{\text{small def.}}$ AND $\% \Delta \phi_{\max}$ ANALOGOUSLY.

Ca	Method	D	$\% \Delta D$	ϕ_{\max} deg.	$\% \Delta \phi_{\max}$
0.05	VEPROST	0.0519	2%	40.17	3.6%
	sdt	0.0509		38.79	
0.1	Newtonian				
	CSF	0.1093	7%	42.75	3.5%
	PROST	0.1012	0.5%	42.73	3.5%
	sdt	0.1017		41.27	
0.1	VECSF	0.1123	10%	33.98	4.1%
	VEPROST	0.1081	6%	33.91	3.9%
	sdt	0.1017		32.63	
0.14	VECSF	0.164	15%	28.78	4%
	VEPROST	0.160	12.6%	28.66	3.6%
	sdt	0.1424		27.675	

$Ca=0.1$ produces $D = 0.108$, $\phi_{\max} = 32.6^\circ$ at $t = 2\dot{\gamma}^{-1}$, as does a finer timestep. The viscoelastic drop is slightly more horizontal because of elastic stresses which push on the drop in the vertical direction, perpendicular to the flow direction.

Numerical results at smaller capillary numbers are closer to the small deformation theory, and deviate the larger the capillary number. This is tabulated in Tab.1. For small deformation, the final state is independent of the split of the total viscosity into solvent and polymer viscosities. For instance, at $Ca=0.14$, Fig.2 shows the case $\eta_s = 1.3$ for total viscosity 10.3. This and $\eta_s = 5.15$ have been checked to evolve to the same D . As Ca increases out of the second-order fluid range, an increase in solvent viscosity enhances extensional stress and the stationary state deforms more. Figure 3 shows the velocity vectors in the x-z cross-section of the drop.

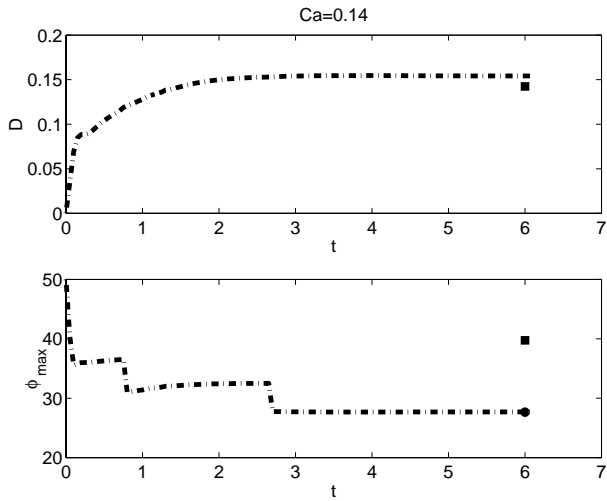


Figure 2. $Ca=0.14$ WITH $\eta_s = 1.3$. THE SQUARES DENOTE NEWTONIAN SMALL DEFORMATION THEORY, AND 'O' DENOTES THE SECOND-ORDER FLUID THEORY. THE INITIAL SHAPE OF THE DROP IS SPHERICAL. THE STATIONARY STATE AT $Ca = 0.1$ WAS ALSO USED AS AN INITIAL SHAPE AND BOTH EVOLVED TO THE CASE SHOWN HERE.

COMPARISON WITH NUMERICAL DATA

In [21], a level-set method is used to compute the deformation of a circular interface in two dimensions with the Oldroyd B model, and a few results for three-dimensions are presented. They find in two dimensions that at $Re = 0.0003, De = 0.4, Ca = 0.24$, viscosity ratio 1, $\eta_s = \eta_p$, a Newtonian drop in a viscoelastic liquid settles to $D = 0.48$. At these parameters, we find in Fig.4 that a three-dimensional evolution settles to $D \approx 0.3, \phi_{max} = 27$ deg.

Figures 5b and 5c of [21] show three dimensional computations at $t=0.9$ and 2.1 for $De = 0.4$ and $Ca = 0.3$. We see a stationary state with $D \approx 0.6, \phi_{max} = 23$ deg. Figure 5 shows the velocity vector plot in the x-z cross-section of the drop at dimensionless $t=3.55$.

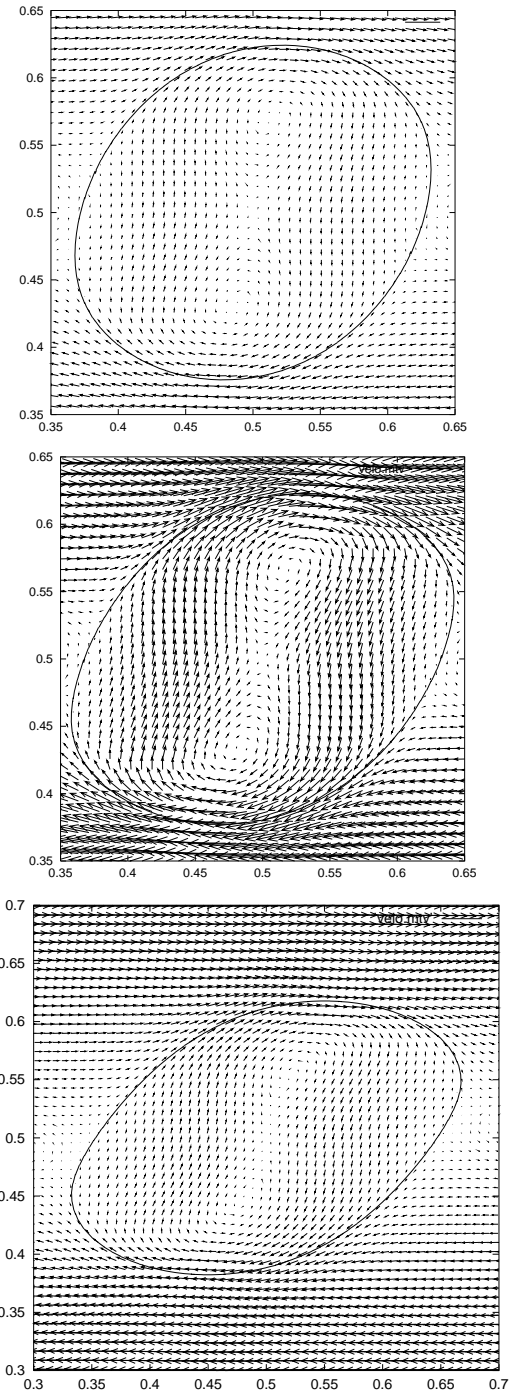


Figure 3. VELOCITY VECTOR PLOTS FOR THE STATIONARY STATE IN THE X-Z CROSS-SECTION OF A THREE-DIMENSIONAL DROP. $Ca = 0.1, 0.14, 0.2$.

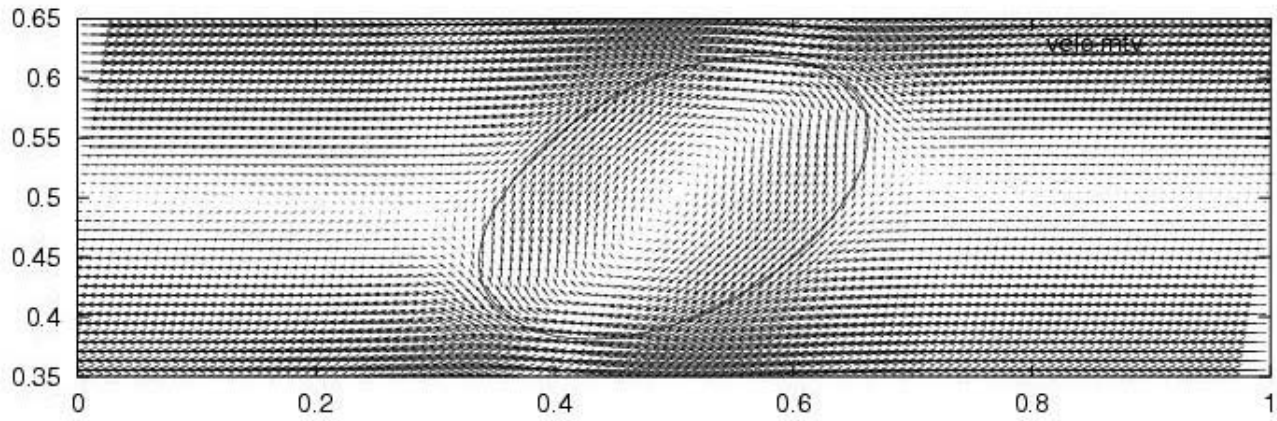


Figure 4. NEWTONIAN DROP IN A VISCOELASTIC LIQUID. VELOCITY FIELD IN A CROSS-SECTION IN THE X-Z PLANE FOR THE STATIONARY STATE. $Re = 0.03$, $\eta_s/\eta_p = 1$, EQUAL VISCOSITY, $We = 0.4$, $Ca = 0.24$.

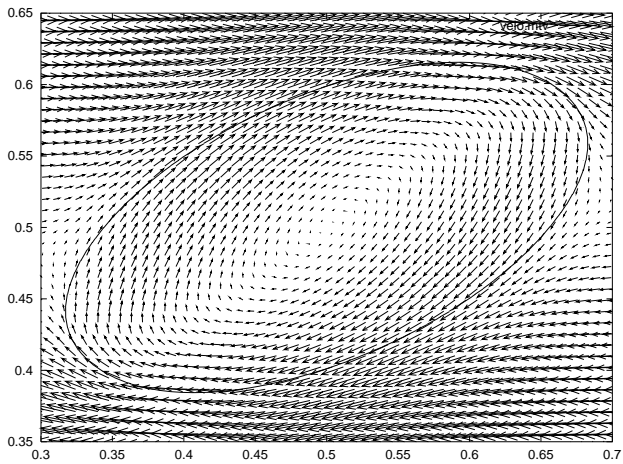


Figure 5. NEWTONIAN DROP IN A VISCOELASTIC LIQUID. VELOCITY FIELD IN THE X-Z CROSS-SECTIONAL PLANE FOR THE STATIONARY STATE. $Re = 0.03$, $\eta_s/\eta_p = 1$, EQUAL VISCOSITY, $We = 0.4$, $Ca = 0.3$.

ACKNOWLEDGMENT

This research is supported by NSF, NCSA and ACS-PRF.

REFERENCES

- [1] D. I. Bigio, C. R. Marks, and R. V. Calabrese. Predicting drop breakup in complex flows from model flow experiments. *International Polymer Processing*, XIII2:192–198, 1998.
- [2] K. S. Sheth and C. Pozrikidis. Effect of inertia on the deformation of liquid drops in simple shear flow. *Computers and Fluids*, 24(2):101–119, 1995.
- [3] M. R. Kennedy, C. Pozrikidis, and R. Skalak. Motion and deformation of liquid drops and the rheology of dilute emulsions in simple flow. *Comput. & Fluids*, 23:251, 1994.
- [4] V. Cristini, J. Blawdziewicz, and M. Loewenberg. Drop breakup in three-dimensional viscous flows. *Phys. fluids*, 10(8):1781–1783, 1998.
- [5] J. Blawdziewicz, V. Cristini, and M. Loewenberg. Critical behavior of drops in linear flows: I. phenomenological theory for drop dynamics near critical stationary states. *Phys. fluids*, 14 (8):2709–2718, 2002.
- [6] J. Blawdziewicz, V. Cristini, and M. Loewenberg. Multiple stationary states for deformable drops in linear stokes flows. *Phys. Fluids*, 15:L37–L40, 2003.
- [7] D. Khismatullin, Y. Renardy, and V. Cristini. Inertia-induced breakup of highly viscous drops subjected to simple shear. *Phys. Fluids*, 15 (5):1351–1354, 2003.
- [8] Y. Renardy. *Direct simulation of drop fragmentation under simple shear*, in *Interfacial Fluid Dynamics and Transport Processes*, Eds. R. Narayanan, D. Schwabe *Lecture Notes in Physics*, pages 305–325. Springer Verlag Berlin ISBN3-540-40583-6, 2003.
- [9] K. Sarkar and W. R. Schowalter. Deformation of a two-dimensional viscoelastic drop at non-zero Reynolds number in time-periodic extensional flows. *J. Non-Newt. Fluid Mech.*, 95:315–342, 2000.
- [10] R. W. Hooper, V. F. de Almeida, C. W. Macosko, and J. J. Derby. Transient polymeric drop extension and retraction in uniaxial extensional flows. *J. Non-Newtonian Fluid Mech.*, 98:141–168, 2001.
- [11] S. Guido, M. Simeone, and F. Greco. Deformation of a Newtonian drop in a viscoelastic matrix under steady shear flow. Experimental validation of slow flow theory. *J. Non-Newtonian Fluid Mech.*, 114:65–82, 2003.
- [12] Y. Renardy and M. Renardy. PROST: a parabolic reconstruction of surface tension for the volume-of-fluid method. *J. Comp. Phys.*, 183(2):400–421, 2002.
- [13] M. Meier, G. Yadigaroglu, and B. L. Smith. A novel technique for including surface tension in PLIC-VOF methods. *European Journal of Mechanics B-Fluids*, 21:61–73, 2002.
- [14] M. Renardy. *Mathematical analysis of viscoelastic flows*. SIAM, 2000.
- [15] F. Greco. Drop deformation for non-newtonian fluids in slow flows. *J. Non-Newtonian Fluid Mech.*, 107:111–131, 2002.
- [16] J. U. Brackbill, D. B. Kothe, and C. Zemach. A continuum method for modeling surface tension. *J. Comp. Phys.*, 100:335–354, 1992.
- [17] F. K. Keller, J. Li, A. Vallet, D. Vandromme, and S. Zaleski. Direct numerical simulation of interface breakup and atomization. In *Proc. Sixth Int. Conf. on Liquid Atomization and Spray Systems*, pages 56–62. Rouen, 1994.
- [18] D. Gueyffier, J. Li, A. Nadim, R. Scardovelli, and S. Zaleski. Volume-of-fluid interface tracking and smoothed surface stress methods for three-dimensional flows. *J. Comp. Phys.*, 152:423–456, 1999.
- [19] R. Scardovelli and S. Zaleski. Direct numerical simulation of free surface and interfacial flow. *Ann. Rev. Fluid Mech.*, 31:567–604, 1999.
- [20] J. Li and Y. Renardy. Numerical study of flows of two immiscible liquids at low Reynolds number. *SIAM Review*, 42:417 – 439, 2000.
- [21] S. B. Pillappakkam and P. Singh. A level-set method for computing solutions to viscoelastic two-phase flow. *J. Comp. Phys.*, 174:552–578, 2001.